

# Harnessing the Potential of EEG in Neuromarketing with Deep Learning and Riemannian Geometry\*

Kostas Georgiadis<sup>1</sup>[0000-0001-9116-4729], Fotis P. Kalaganis<sup>1</sup>[0000-0002-5474-9098], Vangelis P. Oikonomou<sup>1</sup>[0000-0001-7092-8486], Spiros Nikolopoulos<sup>1</sup>[0000-0002-1367-5133], Nikos A. Laskaris<sup>2</sup>[0000-0002-1960-394X], and Ioannis Kompatsiaris<sup>1</sup>[0000-0001-6447-9020]

- <sup>1</sup> Centre for Research & Technology Hellas, Information Technologies Institute (ITI), Thessaloniki, Greece  
<sup>2</sup> AIIA-Lab, Informatics Dept, AUTH, NeuroInformatics.Group, Thessaloniki, Greece  
[georgiaki@csd.auth.gr](mailto:georgiaki@csd.auth.gr)

**Abstract.** Neuromarketing exploits neuroimaging techniques to study consumers’ responses to various marketing aspects, with the goal of gaining a more thorough understanding of the decision-making process. The neuroimaging technology encountered the most in neuromarketing studies is Electroencephalography (EEG), mainly due to its non-invasiveness, low cost and portability. Opposed to typical neuromarketing practices, which rely on signal-power related features, we introduce an efficient decoding scheme that is based on the principles of Riemannian Geometry and realized by means of a suitable deep learning (DL) architecture (i.e., SPDNet). We take advantage of a recently released, multi-subject, neuromarketing dataset to train SPDNet under the close-to-real-life scenario of product selection from a supermarket leaflet and compare its performance against standard tools in EEG-based neuromarketing. The sample covariance is used as an estimator of the ‘quasi-instantaneous’, brain activation pattern and derived from the multichannel signal recorded while the subject is gazing at a given product. Pattern derivation is followed by proper re-alignment to reduce covariate shift (inter-subject variability) before SPDNet casts its binary decision (i.e., “Buy”-“NoBuy”). The proposed decoder is characterized by sufficient generalizability to derive valid predictions upon unseen brain signals. Overall, our experimental results provide clear evidence about the superiority of the DL-decoder relatively to both conventional neuromarketing and alternative Riemannian Geometry-based approaches, and further demonstrate how neuromarketing can benefit from recent advances in data-centric machine learning and the availability of relevant experimental datasets.

**Keywords:** Neuromarketing · Riemannian Geometry · Deep Learning · SPDNet · Electroencephalography · BCIs.

---

\* This work was a part of project NeuroMkt, co-financed by the European Regional Development Fund of the EU and Greek National Funds through the Operational Program Competitiveness, Entrepreneurship and Innovation, under the call RESEARCH CREATE INNOVATE (Project code T2EDK-03661).

## 1 Introduction

Neuromarketing refers to the field of studying consumer behavior by taking advantage of neuroimaging techniques [25, 16]. The conceptualization of neuromarketing by researchers and practitioners is the aftereffect of their efforts to obtain a more thorough understanding regarding the process of consumer decision-making. Neuromarketing’s rapid advancement in the recent years is attributed to the credence that traditional marketing practices, such as focus groups, questionnaires, interviews, and behavioral metrics, are insufficient in capturing the wide variety of aspects involved in consumer behavior. Indeed, traditional practices are cost-effective, scalable, and easy to interpret, however, they lack in terms of generalizability and predictive power. As a matter of fact, participants’ responses may be inaccurate, unreliable, biased, or influenced by others’ opinions (particularly in the case of focus groups) [20].

Electroencephalography (EEG) is the most commonly used neuroimaging method in neuromarketing studies due to its non-invasiveness, portability, cost effectiveness, and high temporal resolution. Although EEG has lower spatial resolution than other neuroimaging technologies, its aforementioned characteristics compensate for this limitation. Neuromarketing is a passive form of Brain-Computer Interface (BCI) that monitors the user’s cognitive states, such as attention, mental workload, and memorization, rather than serving as an alternative communication or control pathway, which is the case for active and reactive BCIs (e.g. [13]).

Typically, EEG-based neuromarketing studies employ signal-power related features of neuroscientific intelligibility in order to examine the consumers’ responses to marketing stimuli. Among those features, the most commonly anticipated indices are those of approach-withdrawal, mental workload, attention, and memorization. In essence approach-withdrawal (AW) is an index that quantifies the hemispheric asymmetry of  $\alpha$  activity in the prefrontal cortex [26]. As AW is a contralateral phenomenon, the increased left or right frontal activity usually indicates the approach and withdrawal effect respectively. Mental workload, which can be interpreted as the effort invested by consumers while making decisions, is quantified by the strength of  $\theta$  activation in the prefrontal/frontal areas [9]. In a similar manner, the memorization process [26] is known to affect the decision making process as the selection of familiar products is more probable. On the contrary, the attention index is studied both at a single-subject level [1] and at a population level [14], with the latter being widely known as inter-subject correlation. Moreover, the emotional aspect is also considered pivotal in the decision making process and consequently several neuromarketing studies have employed emotional indices in this direction [22]. Finally, there are a series of studies that employ fusion techniques to combine the aforementioned indices (e.g. [14, 23]).

Instead of employing naive signal-power features, recent developments in EEG decoding are oriented towards more sophisticated approaches that encapsulate the functional interactions between distinct brain rhythms (i.e. cross-frequency coupling) and the functional dependencies across the distributed cortical networks (by means of various connectivity measures). Among the wide

spectrum of functional connectivity estimators spatial covariance matrix (SCM) stands out as the most computationally efficient, since it inherits the advantage of parallel computation (all pairwise relations are recovered within one step) and can be easily adapted for deriving evolving connectivity patterns. SCMs provide a first glance at the underlying correlation networks while simultaneously incorporate signal power features (i.e., the signal energy levels at the individual sensors are tabulated along the main diagonal of the SCM matrix). By exploiting the fact that SCMs are symmetric and positive definite (SPD), principles of Riemannian Geometry can be employed to study and decode EEG signals in their SCM form. Although typical neuromarketing studies usually rely on statistical tests in order to examine the possibility of predicting consumers' responses from EEG features, our recent study [12] demonstrates that Riemannian geometry holds the potential of achieving state of the art results in the field.

In this study, we aim to advance our previous work [12] by combining the strength of Riemannian Geometry with the increasingly-documented, high predictive power of SPDNet [15], a Riemannian geometry-based deep learning architecture. Although SPDNet has been employed with success in the past for several EEG decoding tasks (e.g., motor imagery [19], emotion recognition [27], etc.), this is the first time that it is exploited in the context of neuromarketing. The employment of SPDNet in our work is enabled by a large-scale dataset that was recently made publicly available by our research group and contains multiple trials of multichannel EEG signals from 42 participants, hence, constituting the employment of deep learning approaches both feasible and fruitful.

As demonstrated in the Results sections, our approach is capable of predicting whether a participant would buy or not a particular product solely from EEG activity. In particular, by adopting a Riemannian alignment procedure [29], we manage to tackle this problem in a subject independent manner, which is in direct contrast with the widely adopted strategy of deploying personalized classifiers. The proposed decoder exhibits state of the art performance, that surpasses both conventional Riemannian geometry approaches and typical neuromarketing approaches. This in turn makes our approach more robust and appropriate for practical applications with the potential of minimizing calibration times.

The remainder of this paper is organized as follows: Sect. 2 describes the selected dataset and the corresponding preprocessing steps, Sect. 3 presents the proposed methodology, Sect. 4 is dedicated to the obtained results, while Sect. 5 discusses the added value and limitations of this work and identifies potential future extensions.

## 2 NeuMa Dataset and Preprocessing

The NeuMa dataset<sup>3</sup> that includes the experimental data of 42 individuals (23 males - 19 females, aged  $31.5 \pm 8.84$ ), while browsing a digital supermarket brochure, was selected for the evaluation of the proposed decoding framework.

---

<sup>3</sup> <https://doi.org/10.6084/m9.figshare.22117124.v3>

Participants were engaged in a realistic shopping scenario, where they had to select (by pressing the left click) the products they intended to buy. In particular, a series of 6 brochure pages were presented to the participants, each including 24 different products belonging to the same product category. Participants could freely browse among the 6 provided brochure pages, with the selection of products being unrestricted both in terms of quantity and total cost. The process resulted in having all products included in the brochure labeled as “Buy” or “NoBuy” depending on whether the product was selected by the participant or not. Prior to the recording process, subjects were thoroughly informed regarding the experiment and provided their written informed consent (approved by CERTH’s Ethical Committee, Ref. No. ETH.COM-68). A more detailed description of the experimental protocol alongside with the corresponding EEG data can be found here [11].

Brain activity was recorded, via 21 dry sensors placed according to the 10-20 International System, namely Fp1, Fp2, Fz, F3, F4, F7, F8, Cz, C3, C4, T7/T3, T8/T4, Pz, P3, P4, P7/T5, P8/T6, O1, O2, A1 and A2 via Wearable Sensing’s DSI 24<sup>4</sup>. The sampling frequency was 300Hz and the impedance for all electrodes was set below 10K $\Omega$  prior to the experiment’s initiation.

Prior to the analysis, the recorded EEG signals were subjected to a two-stage offline preprocessing. Firstly, raw EEG signals were bandpass filtered within [0.5–45] Hz using a 3rd-order zero-phased Butterworth filter. Then, artifactual activity was removed using in sequence Artifact Subspace Reconstruction (ASR) [21] and FORCe [8].

Besides brain activity, ocular activity was also registered using Tobii Pro Fusion eye tracker, with a sampling frequency of 120Hz and the eye movement traces were used for the trial definition/segmentation process. More specifically, a single trial is defined as the time a participant was observing a product, which is equivalent to the time the participant’s gaze was located within the boundaries of each product image. Single trials of duration less than one second were considered insufficient to convey information about  $\delta$  brain rhythm and were consequently discarded [6].

### 3 Methodology

#### 3.1 Riemannian Geometry Preliminaries

Let  $\mathbf{X}_i \in \mathbb{R}^{E \times t}$ ,  $i = 1, \dots, n$  be a single trial EEG response, also referred to as epoch, where  $E$  denotes the number of electrodes and  $t$  the number of time samples. Each  $\mathbf{X}_i$  is accompanied by a label  $y_i \in \{0, 1\}$  that corresponds to two distinct brain states (or performed tasks; in our case corresponding to “Buy”-“NoBuy”). Moving from the time domain, each EEG epoch (assuming zero mean signals) can also be described by the corresponding SCM  $\mathbf{C}_i = \frac{1}{i-1} \mathbf{X}_i \mathbf{X}_i^\top \in \mathbb{R}^{E \times E}$ , where  $(\cdot)^\top$  denotes the transpose operator. By definition and under sufficiently large  $t$  to guarantee a full rank covariance matrix,

<sup>4</sup> <https://wearablesensing.com/dsi-24/>

spatial covariance matrices are symmetric positive definite (SPD) that lie on a Riemannian manifold instead of a vector space (e.g. scalar multiplication does not hold on the SPD manifold).

### 3.2 Riemannian Alignment

While SCMs can provide information rich representations regarding EEG responses, their relative placement over the Riemannian manifold may significantly differ among subjects and even recording sessions of the same subject. In detail, it is possible for a subject’s SCMs to be concentrated at a different area over the same manifold. This problem, usually referred as the covariate shift phenomenon, can significantly harness the performance of deep learning architectures, like SPDNet. To alleviate this problem Zanini et al. [29] proposed a Riemannian alignment process, that in essence re-aligns all SCMs around the same reference point. Consequently, the alignment process requires the identification of a unique reference point in the Riemannian manifold, known as center of mass (or geometric mean) for a given set of SCMs. This point is being identified by minimizing the sum of squared Affine Invariant Riemannian Metric (AIRM)-induced distances [24] (which offers equivalence between the sensor and the source space) as follows, with an iterative process (due to the lack of a closed form solution) and is known as the Karcher/Fréchet mean [3]:

$$\bar{\mathbf{B}} = \underset{\mathbf{P} \in \text{Sym}_s^+}{\text{argmin}} \sum_{i=1}^n \delta^2(\mathbf{C}_i, \mathbf{P}) \quad (1)$$

where  $n$  denotes the number of SCMs,  $\delta$  refers to the AIRM-induced Riemannian distance and  $\mathbf{P}$  being any given point residing on Riemannian manifold.

Finally, once the center of mass has been identified (Eq.1), each SCM can now be re-aligned as follows:

$$\mathbf{C}_i^A = \bar{\mathbf{B}}^{-1/2} \mathbf{C}_i \bar{\mathbf{B}}^{-1/2} \quad (2)$$

### 3.3 The SPDNet Architecture

As its name states, SPDNet is a deep learning architecture designed for processing data that lie on SPD matrices [15]. The SPDNet architecture is based on the idea of representing SPD matrices as points on a Riemannian manifold, which is a space that can be locally treated as an Euclidean space but has a nontrivial global structure. The key idea behind SPDNet is that the convolution and pooling operations are performed on the Riemannian manifold rather than in Euclidean space. This allows the architecture to take into account the intrinsic geometry of SPD matrices when processing them. In the following, the main components of SPDNet are briefly described, while a more detailed description can be found here [15]:

- BiMap Layer: A special type of layer that is designed to preserve the Riemannian structure of SPD matrices while reducing their dimensionality.

- ReEig Layer: A layer designed to improve performance by introducing a non-linearity.
- LogEig Layer: A layer that maps the input SPD matrices onto an Euclidean space.
- A fully connected layer that maps the output of the previous layer to the desired output.

The BiMap layer transforms the input SPD matrices into new SPD matrices by means of a bilinear mapping. In more detail, this layer applies a transformation matrix  $\mathbf{W}$  to the input SPD matrix,  $\mathbf{C}$ , using the bilinear mapping  $\mathbf{WCW}^\top$ . This mapping results in dimensionally reduced SPD matrices. In order to ensure that the resulting output will maintain the SPD property of the input matrix while being dimensionally reduced,  $\mathbf{W}$  is required to be a row full-rank matrix. In essence, the BiMap Layer can be considered as a special type of pooling layer in the SPDnet architecture that uses bilinear pooling to preserve the Riemannian structure of SPD matrices while reducing their dimensionality.

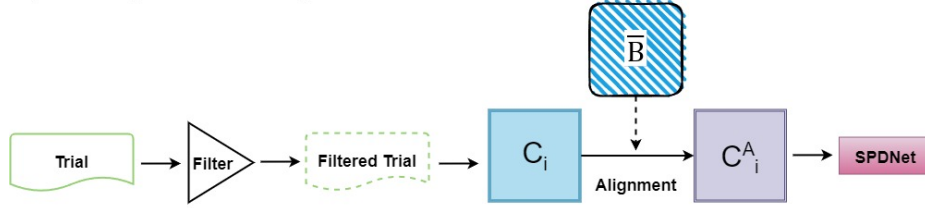
The ReEig layer applies diagonalization to SPD matrices by computing the eigendecomposition of each matrix. However, instead of applying any other non-linear function to the eigenvalues, the ReEig layer applies a ReLU (Rectified Linear Unit) activation function to the eigenvalues. The ReLU function is a commonly used activation function in deep learning that has been shown to improve the performance of neural networks. It simply sets all negative values to zero, while leaving positive values unchanged. In the context of SPD matrices, applying the ReLU function to the eigenvalues has the effect of setting all close-to-zero eigenvalues to a positive value. This has the advantage of enforcing strong positive definiteness on the diagonalized matrices while introducing a non-linearity in order to increase the networks performance.

The LogEig layer performs the logarithmic mapping of the input SPD data. This mapping converts the SPD matrix to a tangent space vector (typically at the Identity matrix) by applying the logarithm operation at the eigenvalues of the SPD matrix. Such an operation can be thought of as a vector that describes how the SPD matrix deviates from the identity matrix. Among the useful properties of the logarithmic mapping (e.g., distance preservation and invariance to affine transformations), it is employed in the context of machine learning since it essentially reduces the SPD manifold to a flat space where Euclidean operation can be deployed.

The fully connected layer in SPDnet is a standard layer that is commonly used in neural networks. However, unlike the fully connected layer in a standard feedforward neural network, the fully connected layer in SPDnet operates on the vectorized form of the input SPD matrices, rather than on the raw feature vectors. In other words, the input to the fully connected layer in SPDnet is a vectorized SPD matrix, which is obtained by flattening the matrix into a vector. The fully connected layer then applies a matrix multiplication to this vector, followed by a bias term and an activation function. The output of this layer is a vector of activations that can be passed to the next layer in the network. The fully connected layer in SPDnet is typically used as the final layer in the network,

where it maps the low-dimensional SPD matrix representations obtained from the previous layers to the desired output space. However, in our setting considering that we are dealing with a classification task, the final layer of the employed architecture is a softmax layer. Finally, we note that the network was trained using a stochastic gradient descent optimization algorithm on Stiefel manifolds, as proposed in [15]

### a) The Proposed Decoding Scheme



### b) The SPDNet Architecture

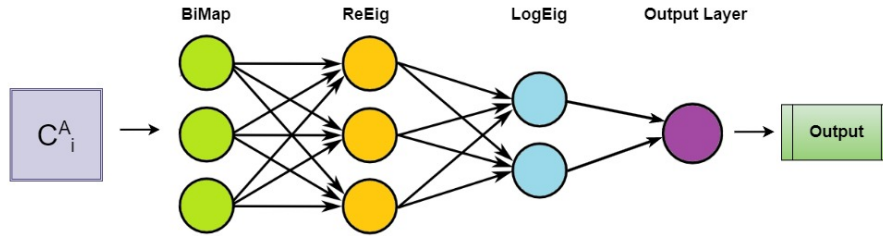


**Fig. 1.** The proposed decoding scheme (a), and the employed SPDNet architecture (b).

## 3.4 The Proposed Decoding Framework for Neuromarketing

The proposed decoder brings the Riemannian related notions and the deep learning architecture of SPDNet described in the previous subsections into the neuromarketing EEG setting. It aims to differentiate the consumers' brain activity between the state during which a product is selected and the opposite state. Fig. 1 graphically illustrates the proposed decoding pipeline and the SPDNet architecture in the upper and lower panel respectively. In some detail, all single trials (i.e. trials from all subjects) are first bandpass filtered within 1-45 Hz, aiming to capture the entire spectrum of brain states (e.g., approach/withdrawal and memorization) that can affect the decision making process [16]. Then SCMs are formulated and re-aligned within the Riemannian manifold as described in subsections 3.1 and 3.2 respectively. Finally, SPDnet is employed to process the corresponding re-aligned SPD representations for each instantiation of the train/test split. It is important to note here, that while for the training data the alignment process can be easily performed using Eq.(2), the process is not

as straightforward regarding the test data, as SCMs arising from the test set must be firstly placed within a pre-learned embedding using the “out of sample extension” algorithm [2].

## 4 Results

The proposed decoder was trained on SCMs derived from Neuma dataset. Its efficiency and efficacy is demonstrated under a dichotomic, “Buy”-“NoBuy”, scenario. A 10-fold cross validation scheme was employed for its thorough evaluation. In this validation scheme, the dataset is being split into ten equal parts and iteratively one part is being used for testing purposes. Additionally, aiming to overcome the barriers imposed by the unbalanced nature of the dataset (i.e. the number of trials labeled as “NoBuy” was higher than the ones labeled as “Buy”) that would harness the performance of any classification scheme, both classes were equally represented before the initiation of the cross validation, by randomly sub-sampling the majority class [5]. This process was repeated 100 times and each time different trials of the “NoBuy” class were included in the train/test split. This approach was followed in order to ensure that the obtained results are neither coincidental nor attributed to the particular selection of the “NoBuy” trials. Hence, the reported classification results correspond to the average of the aforementioned procedure, leading ultimately to a fair evaluation scheme. Concerning the SPDNet hyperparameters we note that it is employed with a batch size of 30 and a learning rate set to 0.01.

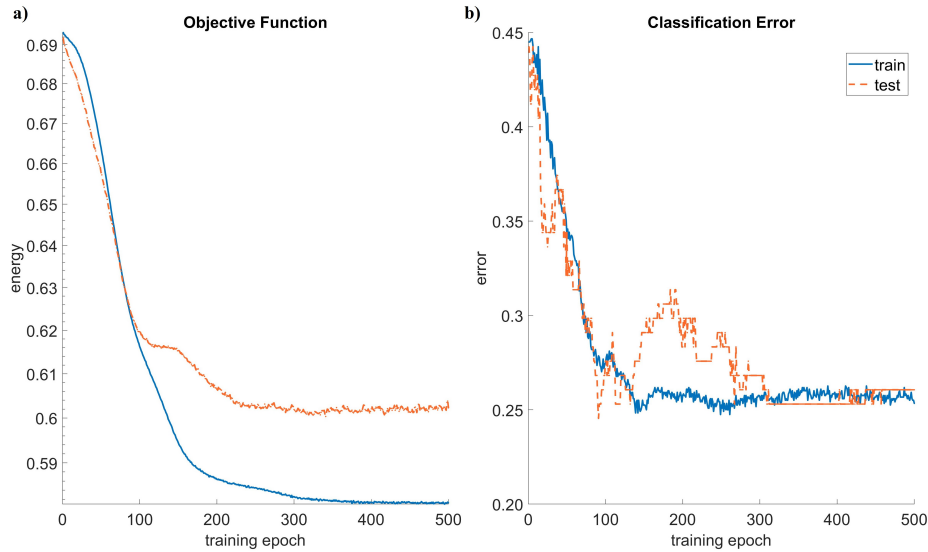


**Fig. 2.** (a) The convergence curve for the proposed decoding scheme and (b) the corresponding error/accuracy curve.

Fig. 2 showcases the accuracy curve and convergence curve of the proposed decoding scheme for an indicative instantiation of the 10-fold cross validation scheme. It is evident that after a few training epochs the decoder’s performance is stabilized between 70% and 75% and that it can converge well approximately within the same number of epochs (i.e. the classification error becomes stable only when the objective function is also stabilized). It is important to note here that similar trends are also observed in the majority of the train/test instantiations, therefore it is safe to assume that approximately 300 epochs would suffice for the training process.

Fig. 3 presents the classification accuracy for the “Buy”-“NoBuy” scenario for the proposed decoder and, in addition, for a classifier that incorporates well-established neuromarketing EEG-based indices and two other popular Riemannian Geometry classifiers [7, 18]. In the former case typical features, like approach-withdrawal and attention, were fused and fed to a Support Vector Machine (SVM), with the approach being referred as EEG-Fusion [14]. In the latter case, the R-kNN (Riemannian k-nearest neighbor: similarly to the classical kNN examines the geodesic distances between SCMs) and the Tangent Space SVM (that classifies SCMs in the Euclidean tangent space delineated by the barycenter of all the SCMs) are used.

It is apparent, that the only approach that can be characterized as competitive to the proposed decoding scheme is the Tangent Space SVM, that reaches a mean accuracy of 67.72% compared to the 72.18% accuracy of the proposed decoder, with the observed difference being statistically significant at a P-value of 0.01. The rest of the approaches employed for comparisons are significantly outperformed by the proposed decoding scheme and their performance cannot be characterized as competitive, considering that both barely surpass the random level. In detail, the EEG-Fusion approach yields an accuracy of 52.75%, while the corresponding accuracy for the R-kNN is 51.96%.

## 5 Discussion

Riemannian Geometry receives continuously increasing attention within the signal processing and machine learning communities, as the provided framework for processing SCMs alleviates a series of problems, like non-stationarity or subject/session variability, encountered in typical signal analytic pipelines. Within the same context, the adaptation of the information-rich SCM descriptors and consequently of Riemannian geometry concepts by the neuroscientific community has led to the design of robust brain decoding schemes.

Despite the well documented potential of the Riemannian Geometry, its application in neuromarketing-related data remains limited. This alongside with the findings of our recent paper [12] that showcased the potential of Riemannian geometry to achieve state of the art performance on neuromarketing data, fueled the present study. In particular, we examined here the conceptual blending of Riemannian geometry with deep learning, as realized in SPDNet with the scope of designing a robust decoding scheme that can detect the preferences of

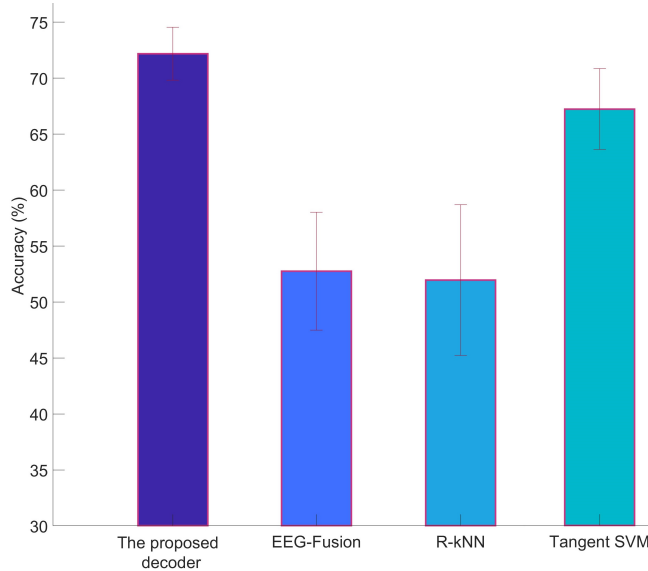


**Fig. 3.** Classification performance in the “Buy”-“NoBuy” scenario.

consumers. The proposed decoder was introduced in the binary setting of the “Buy”-“NoBuy” scenario, with the former referring to products that were selected (i.e. bought) and the latter to the ones that were dismissed. By exploiting an information-rich multi-subject dataset (i.e. a total of 42 subjects), in conjunction with Riemannian alignment process (see subsection 3.2), the feasibility of reliable decoding was demonstrated for the SPDNet. The proposed decoder outperformed standard classifiers operating within the Riemannian framework and a classifier that operates on standard neuromarketing descriptors. Moreover, the added value of proposed decoder stems from the fact that it can be characterized as global, considering that it operates on EEG data from several subjects opposed to previous studies where personalized decoding schemes that lack generalizability are explored (e.g. [9, 12]).

At this point, it is important to note that only one dataset was selected for the validation of the proposed decoder. This decision was imposed by the scarcity of publicly available neuromarketing datasets, as to the best of our knowledge, besides the selected dataset there are only two extra datasets that can be freely accessed [14, 28]. However, both datasets, include a limited amount of trials that constitute the use of SPDNet impractical without employing proper data augmentation procedures (e.g. [17]). Therefore, the generation of artificial data and its incorporation in the proposed decoding pipeline could be considered as potential future extensions of this study.

Another potential future extension of this work could be the reduction of the SCMs’ size, by identifying and selecting the most informative subset of sensors (e.g. [10, 18]) or by combining sensors’ information via approaches like spatial

filters [4]. This could not only lead to improved performance but also to fastest computations, and consequently decreased computational cost. In the same direction, frequency ranges that may carry more discriminative information regarding the SCM formulation can be explored. Finally, exploring the potential of the proposed decoder in a multi-class scenario would be also particularly interesting. The modification steps required to do so seem feasible, as the generated SCMs (for all classes) will reside in a common Riemannian manifold and SPDNet is capable of handling efficiently data arising from multiple classes.

## References

1. Ali, A., Soomro, T.A., Memon, F., Khan, M.Y.A., Kumar, P., Keerio, M.U., Chowdhry, B.S.: Eeg signals based choice classification for neuromarketing applications. A fusion of artificial intelligence and internet of things for emerging cyber systems pp. 371–394 (2022)
2. Bengio, Y., Paiement, J.f., Vincent, P., Delalleau, O., Roux, N., Ouimet, M.: Out-of-sample extensions for lle, isomap, mds, eigenmaps, and spectral clustering. *Advances in neural information processing systems* **16** (2003)
3. Bini, D.A., Iannazzo, B.: Computing the karcher mean of symmetric positive definite matrices. *Linear Algebra and its Applications* **438**(4), 1700–1710 (2013)
4. Blankertz, B., Tomioka, R., Lemm, S., Kawanabe, M., Muller, K.R.: Optimizing spatial filters for robust eeg single-trial analysis. *IEEE Signal processing magazine* **25**(1), 41–56 (2007)
5. Branco, P., Torgo, L., Ribeiro, R.P.: A survey of predictive modeling on imbalanced domains. *ACM computing surveys (CSUR)* **49**(2), 1–50 (2016)
6. Cohen, M.X.: *Analyzing neural time series data: theory and practice*. MIT press (2014)
7. Congedo, M., Barachant, A., Bhatia, R.: Riemannian geometry for eeg-based brain-computer interfaces; a primer and a review. *Brain-Computer Interfaces* **4**(3), 155–174 (2017)
8. Daly, I., Scherer, R., Billinger, M., Müller-Putz, G.: Force: Fully online and automated artifact removal for brain-computer interfacing. *IEEE transactions on neural systems and rehabilitation engineering* **23**(5), 725–736 (2014)
9. García-Madariaga, J., Moya, I., Recuero, N., Blasco, M.F.: Revealing unconscious consumer reactions to advertisements that include visual metaphors. a neurophysiological experiment. *Frontiers in Psychology* **11**, 760 (2020)
10. Georgiadis, K., Adamos, D.A., Nikolopoulos, S., Laskaris, N., Kompatsiaris, I.: A graph-theoretic sensor-selection scheme for covariance-based motor imagery (mi) decoding. In: 2020 28th European Signal Processing Conference (EUSIPCO). pp. 1234–1238. IEEE (2021)
11. Georgiadis, K., et al.: Neuma - the absolute neuromarketing dataset en route to an holistic understanding of consumer behaviour. *Scientific data* (In review)
12. Georgiadis, K., Kalaganis, F.P., Oikonomou, V.P., Nikolopoulos, S., Laskaris, N.A., Kompatsiaris, I.: Rneumark: A riemannian eeg analysis framework for neuromarketing. *Brain Informatics* **9**(1), 22 (2022)
13. Georgiadis, K., Laskaris, N., Nikolopoulos, S., Kompatsiaris, I.: Exploiting the heightened phase synchrony in patients with neuromuscular disease for the establishment of efficient motor imagery bcis. *Journal of neuroengineering and rehabilitation* **15**(1), 1–18 (2018)

14. Hakim, A., Klorfeld, S., Sela, T., Friedman, D., Shabat-Simon, M., Levy, D.J.: Machines learn neuromarketing: Improving preference prediction from self-reports using multiple eeg measures and machine learning. *International Journal of Research in marketing* **38**(3), 770–791 (2021)
15. Huang, Z., Van Gool, L.: A riemannian network for spd matrix learning. In: *Proceedings of the AAAI conference on artificial intelligence*. vol. 31 (2017)
16. Kalaganis, F.P., Georgiadis, K., Oikonomou, V.P., Laskaris, N.A., Nikolopoulos, S., Kompatsiaris, I.: Unlocking the subconscious consumer bias: a survey on the past, present, and future of hybrid eeg schemes in neuromarketing. *Frontiers in Neuroergonomics* **2**, 11 (2021)
17. Kalaganis, F.P., Laskaris, N.A., Chatzilari, E., Nikolopoulos, S., Kompatsiaris, I.: A data augmentation scheme for geometric deep learning in personalized brain–computer interfaces. *IEEE access* **8**, 162218–162229 (2020)
18. Kalaganis, F.P., Laskaris, N.A., Chatzilari, E., Nikolopoulos, S., Kompatsiaris, I.: A riemannian geometry approach to reduced and discriminative covariance estimation in brain computer interfaces. *IEEE Transactions on Biomedical Engineering* **67**(1), 245–255 (2019)
19. Kobler, R., Hirayama, J.i., Zhao, Q., Kawanabe, M.: Spd domain-specific batch normalization to crack interpretable unsupervised domain adaptation in eeg. *Advances in Neural Information Processing Systems* **35**, 6219–6235 (2022)
20. MacKenzie, S.B., Podsakoff, P.M.: Common method bias in marketing: Causes, mechanisms, and procedural remedies. *Journal of retailing* **88**(4), 542–555 (2012)
21. Mullen, T.R., Kothe, C.A., Chi, Y.M., Ojeda, A., Kerth, T., Makeig, S., Jung, T.P., Cauwenberghs, G.: Real-time neuroimaging and cognitive monitoring using wearable dry eeg. *IEEE Transactions on Biomedical Engineering* **62**(11), 2553–2567 (2015)
22. Naser, D.S., Saha, G.: Influence of music liking on eeg based emotion recognition. *Biomedical Signal Processing and Control* **64**, 102251 (2021)
23. Oikonomou, V.P., Georgiadis, K., Kalaganis, F., Nikolopoulos, S., Kompatsiaris, I.: A sparse representation classification scheme for the recognition of affective and cognitive brain processes in neuromarketing. *Sensors* **23**(5), 2480 (2023)
24. Pennec, X., Fillard, P., Ayache, N.: A riemannian framework for tensor computing. *International Journal of computer vision* **66**, 41–66 (2006)
25. Rawnaque, F.S., Rahman, K.M., Anwar, S.F., Vaidyanathan, R., Chau, T., Sarker, F., Mamun, K.A.A.: Technological advancements and opportunities in neuromarketing: a systematic review. *Brain Informatics* **7**, 1–19 (2020)
26. Vecchiato, G., Maglione, A.G., Cherubino, P., Wasikowska, B., Wawrzyniak, A., Latuszynska, A., Latuszynska, M., Nermend, K., Graziani, I., Leucci, M.R., et al.: Neurophysiological tools to investigate consumer’s gender differences during the observation of tv commercials. *Computational and mathematical methods in medicine* **2014** (2014)
27. Wang, Y., Qiu, S., Ma, X., He, H.: A prototype-based spd matrix network for domain adaptation eeg emotion recognition. *Pattern Recognition* **110**, 107626 (2021)
28. Yadava, M., Kumar, P., Saini, R., Roy, P.P., Prosad Dogra, D.: Analysis of eeg signals and its application to neuromarketing. *Multimedia Tools and Applications* **76**, 19087–19111 (2017)
29. Zanini, P., Congedo, M., Jutten, C., Said, S., Berthoumieu, Y.: Transfer learning: A riemannian geometry framework with applications to brain–computer interfaces. *IEEE Transactions on Biomedical Engineering* **65**(5), 1107–1116 (2017)